Environmental Science
Water Research & Technology

ROYAL SOCIETY OF CHEMISTRY

PAPER

View Article Online
View Journal | View Issue



Cite this: *Environ. Sci.: Water Res. Technol.*, 2024, **10**, 1256

# Mechanistic investigation of the photocatalytic activity of PEDOT for aqueous contaminant removal: the role of iron and hydroxyl radicals†

Tahereh Jasemizad, [a] Jenny Malmström [bc] and Lokesh P. Padhye *[a]

In this study, the conducting polymer poly(3,4-ethylenedioxythiophene) (PEDOT) was successfully polymerised through electrochemical (E-PEDOT) and chemical oxidative (C-PEDOT) polymerisation techniques. The photocatalytic reaction mechanism of PEDOT in removing aqueous contaminants, including hexazinone and methylene blue, was investigated with and without the use of Fe(III). An increase in iron concentration during PEDOT irradiation resulted in enhanced degradation of the contaminants. Moreover, E-PEDOT showed up to ~90% removal of contaminants by a combination of adsorption and photocatalysis effects. Hydroxyl radicals played a critical role in the photocatalytic degradation of contaminants using PEDOT, in the presence and absence of iron. This mechanism was proved through coumarin degradation. When evaluating reusability, E-PEDOT showed a decrease in its adsorption behaviour but a consistent photocatalytic activity. Finally, it was revealed that the addition of iron externally or during chemical polymerisation could boost PEDOT performance. Therefore, it is worth considering the implementation of the UV/Fe(III)/PEDOT system, exhibiting remarkable efficacy in eliminating organic contaminants from aqueous solutions.

Received 9th December 2023,
Accepted 18th March 2024

DOI: 10.1039/d3ew00910f

rsc.li/es-water

### Water impact

The study demonstrates the effective removal of an emerging contaminant in water by PEDOT under environmentally relevant conditions, both in the absence and presence of iron, and details the underlying reaction mechanisms. The findings will help the water community focus on iron, an inexpensive and effective photocatalyst, individually and in combination with PEDOT, for larger-scale environmental applications over wide wavelengths of light.

## 1. Introduction

A wide range of processes has been proposed for removing or degrading emerging contaminants from water and wastewater.[1–5] Advanced oxidation processes (AOPs) are widely studied because they are fast, clean, and effective for decontaminating polluted water.[6] UV irradiation, in combination with oxidants or catalysts, as a subset of AOPs, has been considered an effective and practical method to degrade organic compounds in the aquatic environment.[7,8]

Catalysts play a significant role in environmentally friendly and cost-effective processes.[1] In photocatalysis by a semiconductor, charge carriers (electrons ($e^-$) and holes ($h^+$)) are generated upon light absorption.[9–11] The $e^-$ can be excited from the valence band (VB) to the conduction band (CB) by photons. The charge carriers are involved in redox reactions, forming highly reactive oxidative species.[12,13] This technique has attracted great interest in the past few years due to its low operation cost and high efficiency in contaminant remediation.[10–14] Recently, the development of novel photocatalysts that can effectively remove contaminants from water and wastewater has drawn environmental researchers' attention. Moreover, it is necessary to immobilise the photocatalyst to avoid separation difficulties downstream of the treatment.[15]

Conducting polymer (CP)-based photocatalysts, with their suitable physicochemical characteristics, low cost, room temperature operation, and ease of synthesis, have the potential to tackle the problem of water decontamination.[11,16] A low bandgap makes CPs absorb a wide range of wavelengths and thus excellent photocatalysts.[11] Poly(3,4-ethylenedioxythiophene) (PEDOT) is

[a] *Department of Civil and Environmental Engineering, The University of Auckland, Auckland, New Zealand. E-mail: l.padhye@auckland.ac.nz*
[b] *Department of Chemical and Materials Engineering, University of Auckland, Auckland, New Zealand*
[c] *MacDiarmid Institute for Advanced Materials and Nanotechnology, Wellington, New Zealand*

† Electronic supplementary information (ESI) available. See DOI: https://doi.org/10.1039/d3ew00910f

one of the most promising CPs, with a narrow bandgap ($E$ = 1.69 eV), which has previously revealed excellent photocatalytic performance towards organic contaminant degradation.[11,17] PEDOT can be synthesised through different methods, including chemical and electrochemical polymerisation.[18,19]

Iron, naturally abundant, inexpensive, and non-toxic, has been extensively studied for its catalytic role in decomposing peroxides, thereby enhancing the degradation of organic contaminants in water through the formation of reactive species.[20] In the aquatic environment, Fe(III) and Fe(II) are two of the most prevalent metal ions.[21] It has been demonstrated that the presence of dissolved Fe(III) species accelerates the photodegradation of organic compounds in an aqueous solution.[22] This phenomenon can be explained in two ways: (1) Fe(III) absorbs light in a wide range of spectrum; (2) the photoredox process resulting from the excitation of Fe(III) in an aqueous solution leads to an increase in the concentration of Fe(II) and hydroxyl radicals ($^{\bullet}OH$).[22,23] $^{\bullet}OH$ can rapidly react with many organic compounds, leading to their efficient degradation.[4] Furthermore, it is reported that a small amount of iron in the matrix of polymers can significantly enhance the polymer's photocatalytic activity.[24] According to Gogoi *et al.*, using $FeCl_3$ as the oxidant during pyrrole polymerisation resulted in residual $\alpha$-$Fe_2O_3$ in the polypyrrole matrix. The presence of $\alpha$-$Fe_2O_3$ nanoparticles in polypyrrole dramatically enhanced the polymer's photocatalytic activity under visible light.[1]

Fe(III) is used in the chemical polymerisation of PEDOT,[11] and hence it is important to understand its role contribution towards photocatalytic degradation of contaminants using PEDOT. Herein, the photocatalytic efficiency of PEDOT and iron, individually and in combination, towards the photodegradation of organic pollutants was systematically investigated. Hexazinone, an emerging contaminant resistant to photolysis, and methylene blue, a model dye, were selected as target contaminants.[25] The study provides a mechanistic understanding of the photocatalytic ability of PEDOT and distinguishes it from the iron effect.

## 2. Experimental

### 2.1. Chemical reagents

Hexazinone and methylene blue (MB) were purchased from Sigma-Aldrich, New Zealand. Acetonitrile (ACN) and methanol (MeOH) (Sigma-Aldrich, New Zealand) were of HPLC/MS grade (99.9% purity). Iron(III) chloride hexahydrate ($FeCl_3{\cdot}6H_2O$), 3,4-ethylenedioxythiophene (EDOT, 97%), lithium perchlorate ($LiClO_4$), *o*-phenanthroline, hydroxylamine, sodium acetate, sodium hydroxide (NaOH) (98%, pellets) and hydrochloric acid (HCl) were obtained from Sigma-Aldrich, New Zealand. Coumarin and 7-hydroxycoumarin (98%, from Sigma-Aldrich) were used for the identification of $^{\bullet}OH$. Carbon fibre (CF) (ELAT Hydrophilic) was purchased from the Fuel Cell Store (New Zealand). Ultrapure water was obtained from a Millipore Milli-Q® water system (resistivity 18.2 MΩ cm). All other chemicals used in this study were of analytical grade and commercially available.

### 2.2. Electrodeposition of PEDOT on CF cloth (E-PEDOT)

For the electrochemical polymerisation of PEDOT,[37] EDOT was used as a monomer in the polymerisation process in a three-electrode set-up (Gamry). Silver/silver chloride (Ag/AgCl) and stainless-steel were used as a reference electrode (RE) and a counter electrode (CE), respectively. The working electrode (WE) was a carbon fibre cloth that was cut into pieces and cleaned in ACN solution for 15 min in a sonicator (Elma S 100 Elmasonic, bio-strategy). Thereafter, 0.05 M of EDOT monomer was dissolved in 0.1 M $LiClO_4$ electrolyte solution (ACN), which was purged with $N_2$ for 15 min.[38] The polymerisation was conducted in chronoamperometry mode with an applied potential of 1.1 V *vs.* Ag/AgCl for 30 min. A roughly homogenous electrode coating was obtained on both sides of the WE (Scheme 1; step 1). After the reaction, E-PEDOT was characterised to confirm the completion of the reaction, and the immobilised E-PEDOT was washed several times with ethanol and Milli-Q water and dried under ambient conditions. Then, the E-PEDOT electrode was cut into 15 mm × 5 mm size pieces prior to photocatalysis experiments.

### 2.3. Chemical oxidative polymerisation of PEDOT (C-PEDOT)

C-PEDOT in powder form and immobilised on electrospun fibre mat was also tested to compare its photocatalytic

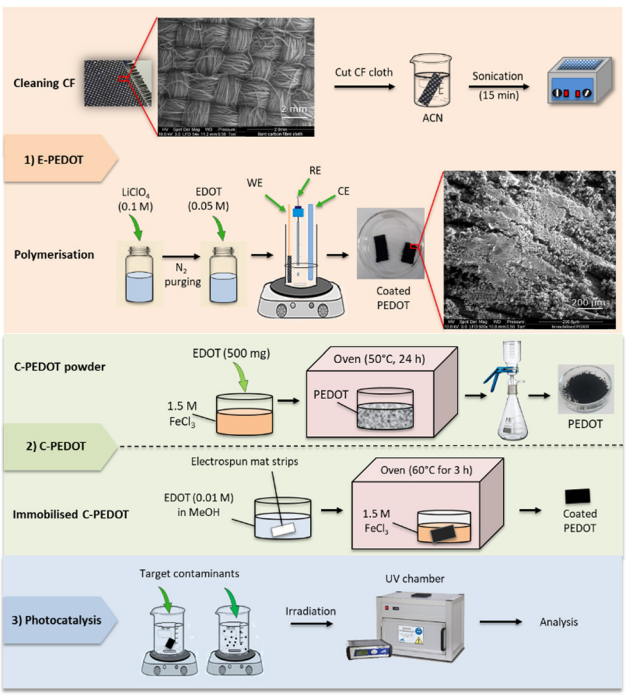


**Scheme 1** The polymerisation of E-PEDOT and C-PEDOT for photocatalysis experiments.

activities with E-PEDOT. The method for the preparation of the electrospun fibre mat and the chemical polymerisation of PEDOT has been previously reported.[11] Briefly, for the preparation of C-PEDOT powder, 500 mg EDOT was added to 10 mL of $FeCl_3$ solution (1.5 M). The solution was stirred for 20 min and kept in an oven at 50 °C for 24 h. Next, the solution was filtered to collect the black PEDOT powder, which was washed several times with Milli-Q water and MeOH to eliminate any remaining salt. Our attempts to coat C-PEDOT on carbon fiber were unsuccessful, as we could not get good PEDOT retention on it. However, the electrospun fiber mat showed good coating of PEDOT. For the preparation of C-PEDOT on the electrospun fiber mat, the strips (5 cm × 13 cm) were soaked in 10 mM EDOT monomer solution in MeOH for 24 h. After drying at room temperature, the dried EDOT-soaked mat was placed in 1.5 M aqueous $FeCl_3$ in an oven (60 °C) for 3 h, followed by rinsing with MeOH to wash away extra salt. The PEDOT coating process was repeated one more time (Scheme 1; step 2). Then, the immobilized C-PEDOT was cut into small 40 mm × 25 mm strips for photocatalytic experiments. Similar sizes of immobilized E-PEDOT and C-PEDOT were initially tested to compare the results.

### 2.4. Characterisation

E-PEDOT was characterised using a Fourier-transform infrared spectrometer (FT-IR INVENIO®, Bruker, Germany) with a scanning wavenumber from 600 $cm^{-1}$ to 4500 $cm^{-1}$, a Raman spectrometer (Raman, LabRAM HR Evolution, HORIBA Scientific, Japan) with 532 nm laser excitation and a scanning range of 900 $cm^{-1}$ to 2000 $cm^{-1}$, and a field emission scanning electron microscope (SEM, FEI Quanta 200 F, USA) attached to an energy-dispersive X-ray spectroscope (EDS) detector.

### 2.5. Photocatalysis experiments

Stock solutions of hexazinone (1 mM), MB (1 mM), coumarin (1000 mg $L^{-1}$ or 6.8 mM), 7-hydroxycoumarin (10 mg $L^{-1}$ or 0.062 mM), and $FeCl_3$ (1 M) were prepared in Milli-Q water and stored in amber glass bottles in the fridge (4 °C) until use. A 10 mL reaction solution containing 5 μM hexazinone, 16 μM MB, or 0.42 μM coumarin with and without PEDOT strips and iron was used for experiments. All batch experiments were carried out at room temperature (25 °C). Most of the experiments were performed at pH ~6.5 to have a similar condition as the real-world samples except for the effect of pH experiments in which pH was adjusted using 0.1 M NaOH and HCl and measured with a pH meter (HACH, HQ40d). In this study, only the effect of initial pH was tested. Each experiment was carried out in duplicate except for pH and adsorption/desorption experiments, which were performed in triplicate. Error bars in all the graphs illustrate the maximum and minimum measurements for replicates.

All the irradiation experiments were carried out in a UV chamber (Opsytec Dr. Grobel, Germany) equipped with eight 15 W low-pressure lamps (Philips Co., Japan) that emit light primarily at 254 nm (UVC), 313 nm (UVB), and 352 nm (UVA). The intensity of each lamp was measured by radiometric sensors. The highest light intensity for UVC, UVB, UVA, and visible (daylight) is determined to be approximately 20, 16.80, 13.60, and 8 mW $cm^{-2}$, respectively. For photocatalysis experiments, E-PEDOT and C-PEDOT were dipped in the contaminant solution (10 mL) just prior to the irradiation (Scheme 1; step 3). In addition, adsorption experiments were carried out under conditions similar to photocatalysis but in the absence of light. To understand the role of iron alone and together with PEDOT, various concentrations of $FeCl_3$ were added to MB and hexazinone solutions under different wavelengths and in the absence of light (adsorption). Finally, the samples were taken at predetermined intervals of time to be analysed for the residual concentrations of hexazinone and MB. The adsorption/photodegradation (%) was calculated according to the following formula:

$$\text{Adsorption/Photodegradation (\%)} = \frac{C_0 - C}{C_0} \times 100 \quad (1)$$

where $C_0$ and $C$ are the initial and residual concentrations of contaminants, respectively.

### 2.6. Analytical methods

The quantification of aqueous hexazinone, coumarin and 7-hydroxycoumarin was performed through liquid chromatography–tandem mass spectrometry (LC–MS/MS) (Shimadzu, Japan), using a 150 μL aliquot of sample. The separation was done on a 2.1 mm × 100 mm, 3.5 μm, Eclipse Plus C18, Agilent column. The details of LC–MS/MS conditions were described previously[25,26] (Text S1†). MB was quantified through a UV-vis spectrophotometer (UV-2700, Shimadzu) using a photometric method at 664 nm. Microwave plasma atomic emission spectrometer (MP-AES, Agilent Technologies 4210) was used to measure the residual amount of iron in samples. Total iron and Fe(II) concentrations were measured through the *o*-phenanthroline spectrophotometry method.[27,28] *o*-Phenanthroline can specifically and rapidly react with Fe(II) and form a stable orange complex with the maximum absorbance at $\lambda$ = 510 nm. Fe(III) was then calculated by taking the difference between the total iron and Fe(II).

## 3. Results and discussion

### 3.1. Role of iron without PEDOT

The effect of Fe(III) was tested on the degradation of hexazinone and MB under different irradiation sources. The control experiments were performed in the presence of iron in the dark and in the absence of iron under irradiation. Very low degradation, <10% for MB (Fig. 1A–D) and <5% for hexazinone (Fig. 1F–I), was observed after 1 h of irradiation with all types of lights in the absence of iron at near-neutral

 

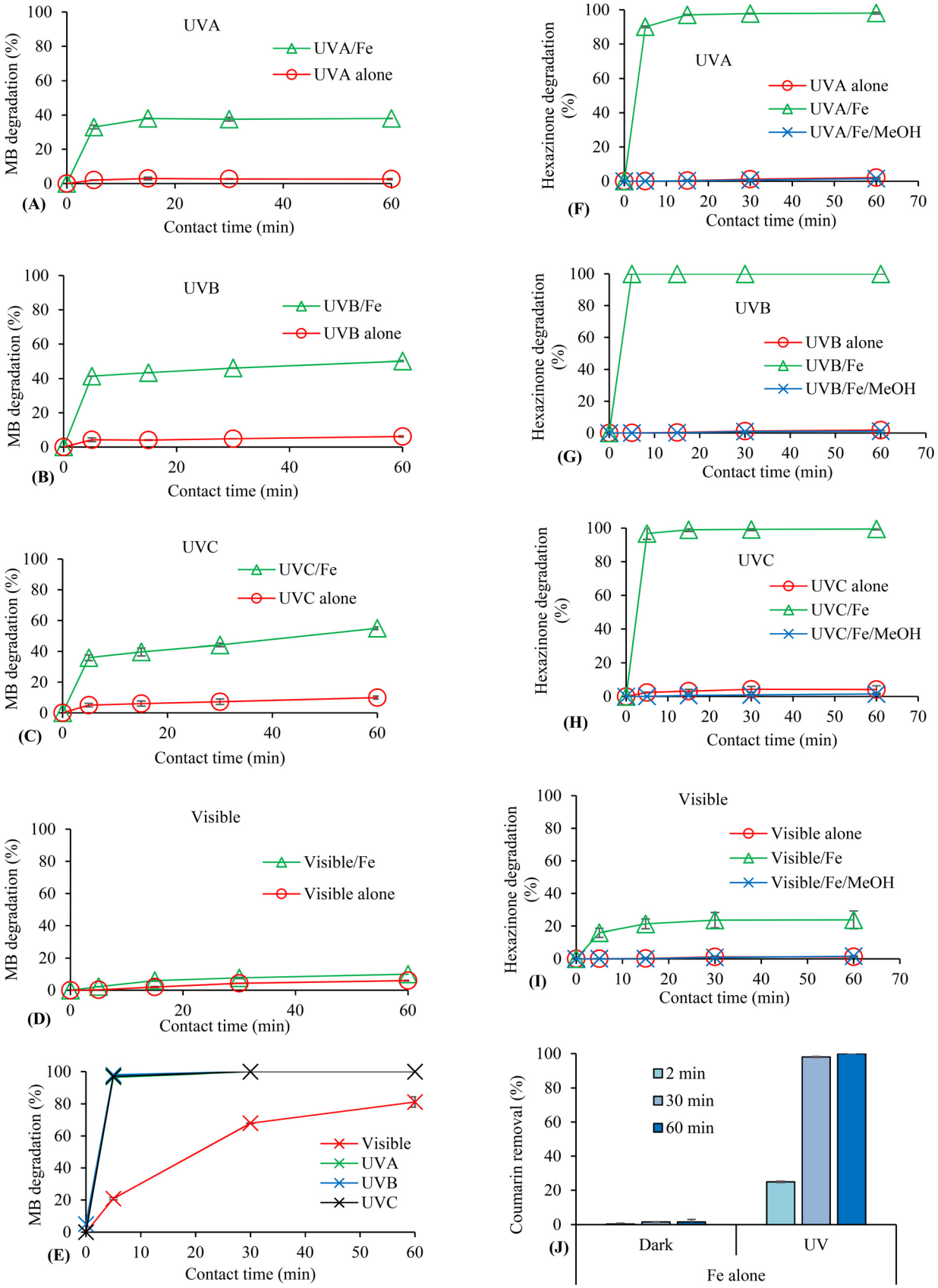


**Fig. 1** Effect of 0.05 mM Fe(III) on the photodegradation of MB exposed to UVA (A), UVB (B), UVC (C), and visible (D) lights. Effect of 0.5 mM Fe on MB photodegradation under all types of light sources (E). Effect of Fe in the presence and absence of MeOH on the photodegradation of hexazinone exposed to UVA (F), UVB (G), UVC (H), and visible (I) lights. Coumarin removal under UVC in the presence of 0.05 mM $FeCl_3$ (J) (experimental conditions: $[MB]_0$ = 15.6 μM, $[hexazinone]_0$ = 5 μM, $[Fe(III)]_0$ = 0.05 and 0.5 mM, $[MeOH]_0$ = 0.5 mM, pH ~6.5).

pH, while no degradation was observed in the presence of iron in the dark.

On average, 37% degradation of MB was observed after 5 min exposure to UVA, UVB, and UVC irradiation in the presence of 0.05 mM Fe(III) with only a slight increase in degradation from 5 to 60 min (Fig. 1A–C). On the other hand, MB degradation rate under visible light irradiation and 0.05 mM Fe(III) was less than 10% (Fig. 1D). In the presence of a higher concentration (0.5 mM) of Fe(III), >95% degradation of MB was observed at 5 min under all types of irradiation sources except for visible light. However, the degradation enhanced from ~20% to 81% under visible light by increasing the reaction time from 5 to 60 min (Fig. 1E).

It is known that $^{\bullet}OH$ can be generated through a simple photochemical reaction between Fe(III) and water according to the following equation:[29,30] Note that this is different from the photo-Fenton reaction which involves hydrogen peroxide.

$$Fe(III) + H_2O \xrightarrow{h\nu} Fe(II) + H^+ + {}^{\bullet}OH \quad (2)$$

To verify the role of $^{\bullet}OH$, hexazinone photodegradation was investigated in the presence of 0.05 mM Fe(III) using methanol, a well-known $^{\bullet}OH$ scavenger.[31] The results are displayed in Fig. 1F–I. Hexazinone photodecomposition was >90% under UVA, UVB, and UVC after 5 min reaction time (Fig. 1F–H). Moreover, it increased from about 16% to 24% under visible light illumination by increasing the reaction time from 5 to 60 min (Fig. 1I). The photodecomposition was completely inhibited by 0.5 mM methanol under all irradiation sources, verifying the important role of $^{\bullet}OH$ in the photodegradation of the contaminant. A similar result was observed for the photodegradation of MB in the presence of MeOH (Fig. S1†). Moreover, since coumarin has been previously used as a probe for its effective reaction with $^{\bullet}OH$ to form umbelliferone,[11] the removal of coumarin and the formation of its by-product, 7-hydroxycoumarin, were investigated at different times to prove $^{\bullet}OH$ generation.[32] Coumarin degradation under UVC in the presence of 0.05 mM $FeCl_3$ enhanced from about 25% to 100% by increasing the time from 2 to 60 min (Fig. 1J). The formation of 7-hydroxycoumarin in very low concentrations was detected only under UV irradiation but not in the dark.

Only a few studies have investigated the photodegradation of contaminants from aqueous solutions using ferric salts without using other oxidants such as $H_2O_2$.[28,29,33,34] The degradation of tetracycline under UV irradiation in the presence of $FeCl_3$ showed the maximum degradation rate at 20 μM Fe(III), which corresponded to a 1 : 1 molar ratio of tetracycline to Fe(III).[27]

In the current study, different concentrations of Fe(III) were used for the degradation of 5 μM hexazinone to understand the influence of varying ratios of Fe(III) : contaminant (Fig. 2A). However, the results demonstrated only 7% photodegradation with a 1 : 1 molar ratio of Fe(III) : hexazinone. Hexazinone degradation increased from about 4% to 100% by increasing the molar ratio of Fe(III) : hexazinone from 1 : 5 to 10. As can be seen from Fig. 2A, an increase in the rate constants of hexazinone photodegradation was observed by increasing Fe(III) concentration. This increase can be due to the formation of a higher amount of $^{\bullet}OH$ in the system. To calculate the degradation rate constant ($k$ ($h^{-1}$)), a pseudo-first-order kinetic model was used (eqn (3)) with regression coefficient ($R^2$) >0.89 and the results for different ratios of Fe(III) : hexazinone are shown in Fig. 2A.

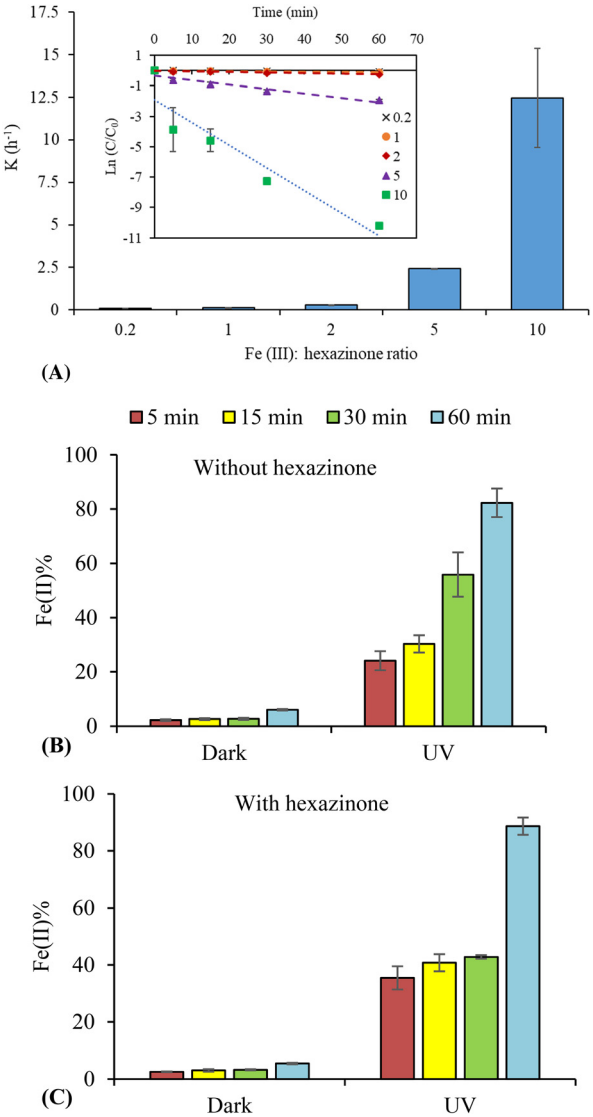


Fig. 2 (A) Effect of different ratios of Fe(III) : hexazinone on the photodegradation of hexazinone with hexazinone degradation kinetics in the presence of different Fe(III) : hexazinone ratios (experimental conditions: $[hexazinone]_0$ = 5 μM, pH ~6.5, exposure time = 5 to 30 min, UVC intensity = 20 mW $cm^{-2}$), $k$ is the degradation rate constant. Effect of time on the conversion of Fe(III) to Fe(II) in (B) Milli-Q water and (C) hexazinone solutions (experimental conditions: $[hexazinone]_0$ = 5 μM, $[Fe(III)]_0$ = 0.074 mM, Fe(III) : hexazinone ratio ~15 : 1, pH ~6.5, UVC intensity = 20 mW $cm^{-2}$). Data are presented as the average of formed Fe(II) (%) ± standard deviation ($N$ = 2).

$$\mathrm{Ln}\left(\frac{C}{C_0}\right) = -k_{obs}\cdot t \quad (3)$$

where $C_0$ is the initial concentration of contaminants and $C$ is the concentration after degradation at time $t$ (h). $k_{obs}$ is the pseudo-first-order reaction rate constant ($h^{-1}$).

The results of our study and most of the literature suggest that using ferric salts alone under visible light or UV irradiation can be an efficient technique for the degradation of organic contaminants and should be further researched.

To investigate the conversion of Fe(III) to Fe(II), the experiments were conducted in the dark and under irradiation, in the presence and absence of hexazinone at near-neutral pH. Fig. 2B and C show the percentage of Fe(II) formed from 0.074 mM Fe(III) in the presence and absence of 5 μM hexazinone in the dark and under irradiation. The concentration of Fe(III) (0.074 mM) was chosen for the complete degradation of hexazinone. The results showed that Fe(II)% was very low in the dark while it was higher under irradiation (Fig. 2B and C), confirming a reduction of Fe(III) to Fe(II) under UVC irradiation. In addition, similar results were observed for samples with and without hexazinone, demonstrating that Fe(II) formation was not affected by the presence of hexazinone in the aqueous solution.

Similar to these results, the photodegradation of tetraacetylethylenediamine[35] and diuron[20] in the presence of Fe(III) showed a higher formation of Fe(II) under 365 nm irradiation than in the dark. These studies also found that by the addition of ˙OH scavengers, the degradation of the contaminants was inhibited, but there was still a rise in the formation of Fe(II) over time. This could explain the critical role of ˙OH in the photodegradation of these organic compounds.

Moreover, in the present study, the continuous increase of Fe(II)% over time resulted only in a slight increase in the contaminants' photodegradation (Fig. 1), which is probably due to the reaction of excess Fe(II) with ˙OH, leading to a decrease of available ˙OH for the contaminants.[27,33] To prove this scavenging effect of Fe(II), De Laat *et al.* added different Fe(II) concentrations (0–100 μM) into the Fe(III) (20 μM)/UV system and found a decrease in the oxidation rate of atrazine with an increase in Fe(II) concentration.[33] It indicates that only ˙OH is responsible for the degradation of hexazinone and MB in the Fe(III)/UV system. Brand *et al.* also found that the concentration of Fe(II) reached a plateau after about 4 h irradiation, confirming the oxidation of Fe(II) into Fe(III).[35] However, the plateau in Fe(II)% was not observed in the present study as experiments were no longer than 1 h of UV exposure.

On the other hand, Yao *et al.* assumed that the photodegradation of tetracycline under UV irradiation was initiated by the generation of Fe(III)–tetracycline complexes, after which ligand to metal charge transfer resulted in the oxidation of tetracycline and the reduction of Fe(III) to Fe(II). Subsequently, Fe(II) could be oxidised to Fe(III) by dissolved $O_2$.[27] In the present study, the formation of the hexazinone–Fe(III) complex seems unlikely because the results showed similar Fe(II)% for the solutions with and without hexazinone (Fig. 2B and C). In summary, OH radicals, produced in the Fe(III)/UV system, are the only reactive species involved in the degradation of hexazinone. However, Fe(II) formed from Fe(III) reduction under irradiation, which increases over time, can react with ˙OH and hence reduce its efficiency at higher reaction times. The quantum yield of ˙OH in the UV/Fe system under 254 nm at pH 6 has been reported to be 0.0046.[36]

### 3.2. Effect of PEDOT

Considering the use of iron as an oxidant during the chemical polymerisation of CPs and its role in ˙OH formation under irradiation, the use of iron may lead to a misinterpretation of the polymers' photocatalytic activities due to the formation of more ˙OH. Therefore, in this study, the photocatalytic activity of E-PEDOT, polymerised without the use of iron, was compared to that of C-PEDOT, polymerised with iron.

#### 3.2.1. Effect of E-PEDOT

*3.2.1.1. Characterisation of E-PEDOT.* E-PEDOT was deposited on the surface of CF cloth through electrochemical polymerisation in the chronoamperometry mode (Fig. S2A†). The polymerisation potential of 1.1 V was determined by the polymerisation in cyclic voltammetry (CV) mode (Fig. S2B†). Moreover, the polymerisation potential of 1.1 V in the chronoamperometry mode was chosen based on the CV results.

The characterisation results of bare CF cloth and E-PEDOT are shown in Fig. 3. As can be seen from Fig. 3A and B, the FT-IR spectra of controls, $LiClO_4$ and EDOT on CF are identical to that of bare CF cloth. In addition, the FT-IR spectra of the coated E-PEDOT were similar before and after irradiation (Fig. 3C). For E-PEDOT coated on carbon fibre, the bands at 1513 and 1321 $cm^{-1}$ are attributed to the asymmetric stretching mode of carbon–carbon double bonds (C═C) and the inter-ring stretching mode of C–C, respectively. The bands at 1191, 1137, and 1047 $cm^{-1}$ are assigned to C–O–C bond stretching in ethylenedioxy. The bands at 972, 914, 821, and 682 $cm^{-1}$ can be the characteristic bands of C–S–C bond stretching in the thiophene ring.[11,37,38] The Raman spectra for the bare CF represent mainly two bands at 1353 and 1589 $cm^{-1}$ [39] (Fig. 3D). The Raman spectra of E-PEDOT before and after irradiation are similar (Fig. 3E and F). The band located at 993 $cm^{-1}$ is due to the deformation of the oxyethylene ring. The bands around 1123 and 1275 $cm^{-1}$ can be attributed to C–O–C deformation and Cα–Cα′ inter-ring stretching, respectively. The bands at 1370, 1448 and 1509 $cm^{-1}$ can be assigned to the Cβ–Cβ′, Cα–Cβ (–O) and asymmetric Cα–Cβ stretching, respectively.[11,40] The SEM images of bare CF cloth before and after coating with E-PEDOT are shown in Fig. 3G and H, respectively. As can be seen from the figures, the CF cloth coated with E-PEDOT shows a rough surface on

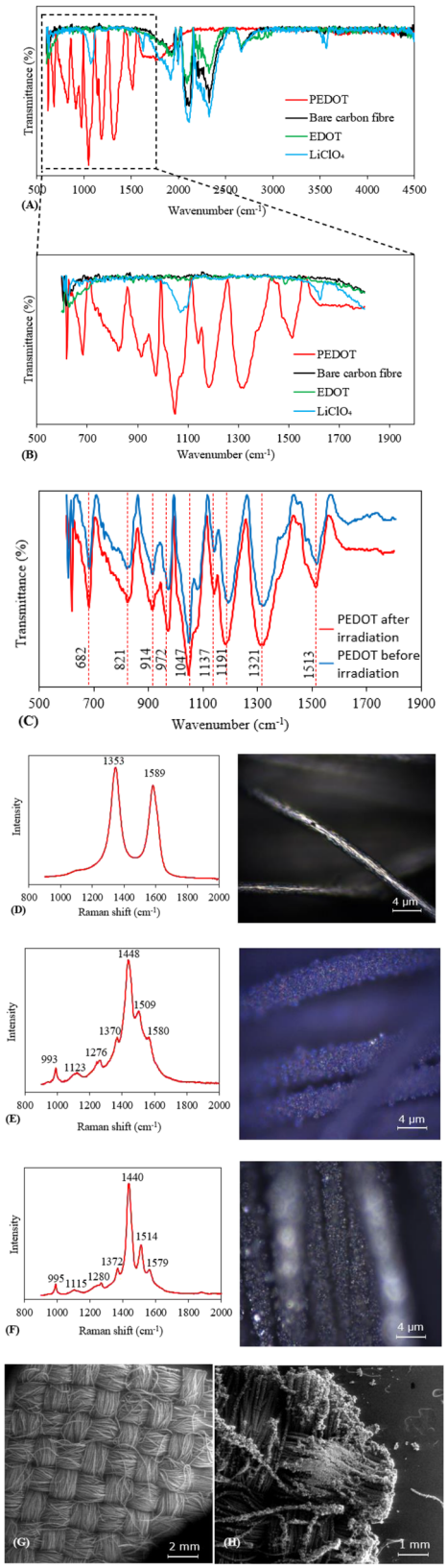


Fig. 3 FT-IR spectra of the bare carbon fibre cloth, controls (EDOT and $LiClO_4$), and E-PEDOT (A) full scale, (B and C) magnified; Raman spectra of (D) bare carbon fibre with its OM image, (E) immobilised E-PEDOT before irradiation with its OM image, (F) immobilised E-PEDOT after irradiation with its OM image; SEM images of (G) bare carbon fibre cloth and (H) immobilised E-PEDOT.

the fibre. These characterisation methods confirm the successful immobilisation of E-PEDOT on the surface of CF cloth.

*3.2.1.2. Adsorption and desorption of contaminants on E-PEDOT.* Prior to photocatalytic experiments in the presence of E-PEDOT, adsorption (24 h) and desorption (24 h) studies were performed with 5 μM hexazinone at pH ~6.5 in the dark. Although the control experiments showed negligible adsorption properties for CF cloth, about 63% mass of hexazinone was adsorbed onto E-PEDOT after 24 h adsorption. Subsequently, ~20% mass of hexazinone was desorbed from PEDOT into fresh Milli-Q water in 24 h. Due to the insignificant desorption, the sample was sonicated for 2 h; however, still, only an additional 7% mass of hexazinone was desorbed into the solution (Fig. 4). Similar experiments were carried out for 15.6 μM MB, and similar results were observed (Fig. S3†). This low desorption can be due to a strong adsorption bonding between the pollutants and PEDOT, which makes adsorption on E-PEDOT relatively irreversible.

*3.2.1.3. Effect of pH on photocatalytic activity of E-PEDOT.* To investigate the performance of E-PEDOT, the PEDOT strips were first dipped into a 5 μM hexazinone solution at different pH values. The control experiments showed similar results for CF/UV and UV alone, demonstrating no photocatalytic activity for the CF cloth (Fig. S4†). The role of initial pH is critical in the degradation of organic compounds. It can determine the compound dissociation (*e.g.*, the ionic form of a compound might be favourable for degradation in some cases). In addition, surface interaction can be influenced by pH, which depends on the point of zero charge of the material. For example, catalyst charge may promote the adsorption of contaminants, leading to their decomposition at the surface of the catalyst, where $h^+$ and/or reactive oxygenated species are generated.[41] For pH experiments, adsorption in the dark was first carried out for 3 h to evaluate the adsorption performance of the E-PEDOT strips. Thereafter, hexazinone photodegradation in the

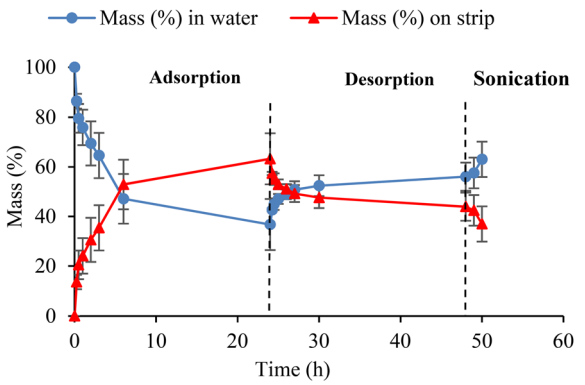


Fig. 4 Adsorption and desorption of hexazinone on E-PEDOT (experimental conditions: $[hexazinone]_0$ = 5 μM, pH ~6.5); data are presented as the average of mass (%) adsorbed or desorbed ± standard deviation ($N$ = 2).

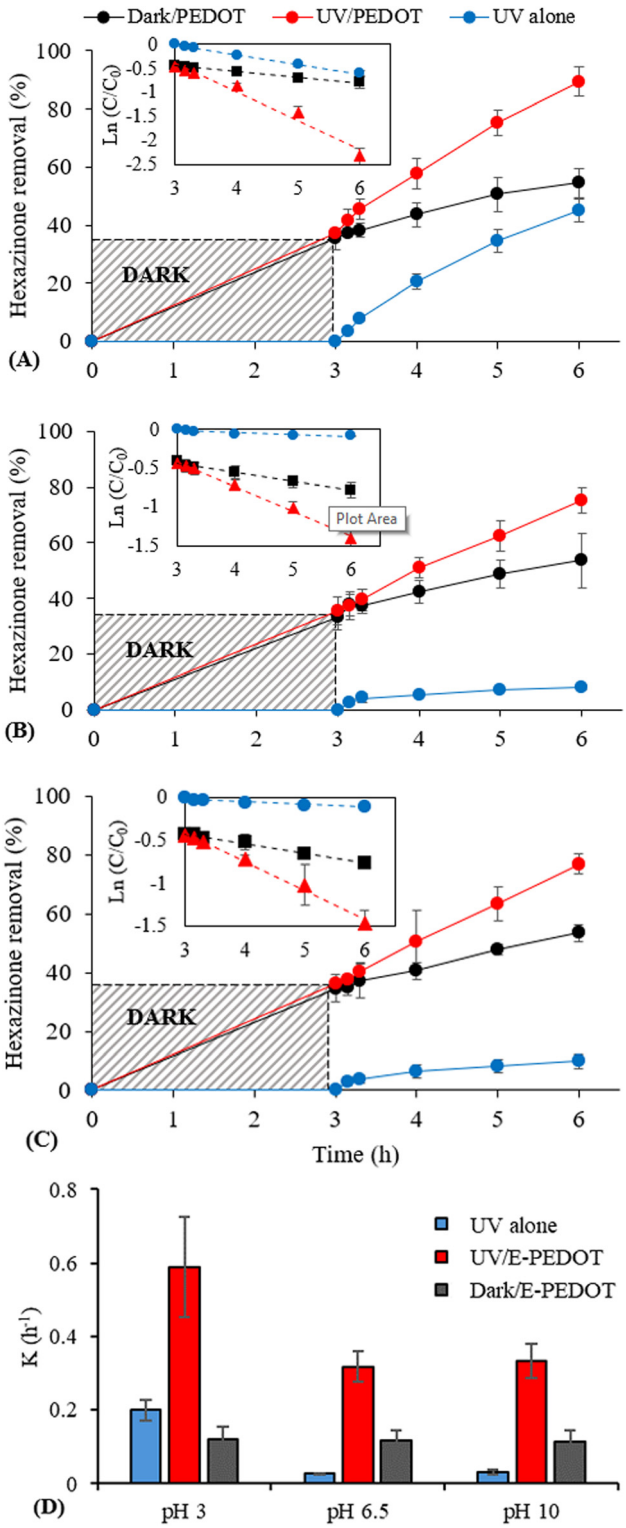


Fig. 5 Hexazinone removal (%) and kinetics at different pHs; (A) pH = 3, (B) pH ~6.5, (C) pH = 10, and (D) hexazinone degradation rate constants at different pHs (experimental conditions: $[\text{hexazinone}]_0$ = 5 μM, UVC intensity = 20 mW $cm^{-2}$).

presence of E-PEDOT under UVC irradiation with 20 mW $cm^{-2}$ intensity was performed. E-PEDOT adsorption efficiency was also monitored under identical conditions but in the dark. The results for hexazinone removal (%) and pseudo-first-order kinetic models at different pHs are demonstrated in Fig. 5A–C. Moreover, hexazinone degradation rate constants ($k$ ($h^{-1}$)) at different pHs (Fig. 5D) were calculated using a pseudo-first-order kinetic model (eqn (3)) with regression coefficient ($R^2$) >0.9 (Fig. 5A–C).

As shown in Fig. 5A–C, approximately 35% adsorption occurred in the first 3 h and reached about 53% after another 3 h in the dark at all different pHs. Hexazinone photodegradation in the absence of photocatalyst (UV alone) ($k$ ~0.2 $h^{-1}$) was favoured under acidic pH, and therefore higher degradation of hexazinone was observed under this condition in the UV/E-PEDOT system ($k$ = 0.59 $h^{-1}$) (Fig. 5D). The differences in photodegradation between semi-neutral and basic pHs in the UV alone and the UV/E-PEDOT systems were insignificant. Although hexazinone photodegradation in the absence of E-PEDOT was very low (<10% after 3 h irradiation) under semi-neutral and basic pH, hexazinone photocatalytic degradation in the presence of E-PEDOT increased from 35% to about 75% after 3 h irradiation ($k$ ~0.32 $h^{-1}$). Hence, approximately 35% (pH 3) and 22% (pH 6.5 and 10) degradation of hexazinone can be considered as a photocatalytic activity of E-PEDOT after 3 h exposure time.

According to Weerakoon *et al.* (2023), the pH-dependent photolysis of a compound under UV probably arises from two factors: type and intensity of UV and molar absorption coefficient of the organic contaminant.[42] Since the UV type and intensity was same, the higher degradation of hexazinone at acidic pH (Fig. 5A) can be attributed to combination of hexazinone being in neutral form and higher quantum yield. It is reported that in their neutral state, molecules exhibit strong light absorption and heightened photochemical reactivity, leading to enhanced removal efficiency.[8] The control experiments for the effect of UV on the adsorption properties of E-PEDOT were conducted through 3 h irradiation of E-PEDOT strips in Milli-Q water. It was followed by dipping those strips in 10 mL hexazinone solution (5 μM) for different reaction times in the dark. No change was observed in the adsorption behaviour of E-PEDOT. The effect of initial pH on the photocatalytic performance of some PEDOT-based photocatalysts has been previously reported.[11,43,44]

The combination of adsorption and photocatalysis of contaminants makes E-PEDOT highly effective. Semiconductor photocatalysts with heterogeneous nature are capable of adsorbing contaminants on their surface. Hence, adsorption can be involved with photocatalytic degradation. Although photocatalytic degradation is usually the dominant mechanism, the percentage of the effectiveness of these mechanisms depends on the composites applied for photocatalyst preparation.[9,45,46] In the present study, the adsorption, with 53% removal efficiency, was dominant, while the photocatalytic activity of E-PEDOT played a secondary role, with about 22% removal after 6 h at semi-neutral pH (Fig. 5B). The adsorption of aromatic compounds, such as hexazinone and MB, generally depends on π–π bond

interactions between their aromatic rings and the surface of the adsorbent, in this case, E-PEDOT.[41,47]

*3.2.1.4. Effect of ˙OH scavenger on E-PEDOT efficiency.* Photocatalysis involves the formation of charge carriers ($e^-$ and $h^+$) and their catalytic reactions. A good photocatalytic performance is highly related to the effective separation of photoexcited $e^-/h^+$ pairs produced after the excitation of photocatalysts.[17] Due to the involvement of many reactive species in the photocatalytic oxidation process, it is useful to examine the effect of scavengers on the photocatalytic degradation of contaminants to elucidate the involved reactive mechanisms.[48]

In this study, the effect of MeOH as ˙OH scavenger on E-PEDOT efficiency for degradation of hexazinone was investigated owing to the critical role of this radical (Fig. 6A and B). The adsorption experiments were conducted for 3 h in the dark followed by photocatalytic degradation under irradiation for up to 3 h. The degradation rate of hexazinone ($k$ = 0.32 $h^{-1}$) was hindered in the presence of 0.5 mM MeOH ($k$ = 0.14 $h^{-1}$), highlighting the role of ˙OH involved in the photodegradation in the presence of E-PEDOT. Similar results were observed using MB (data not shown). Since the photodegradation results in the UV/PEDOT/MeOH system ($k$ = 0.14 $h^{-1}$) were similar to that in the Dark/PEDOT system ($k$ = 0.12 $h^{-1}$), it confirms the important role of ˙OH in the UV/PEDOT system.

The effect of different scavengers on PEDOT photocatalytic activity has been investigated and reported in the literature.[11,17,49] These studies suggested the important role of charge carriers ($e^-$ and $h^+$) and radicals (˙OH and $O_2^{\bullet-}$) in the photocatalytic mechanism of PEDOT. In the present study, we hypothesised that PEDOT irradiation produces $e^-$ and $h^+$. Later, ˙OH, responsible for the contaminant photodegradation, can be generated *via* a series of redox reactions (Scheme 2).

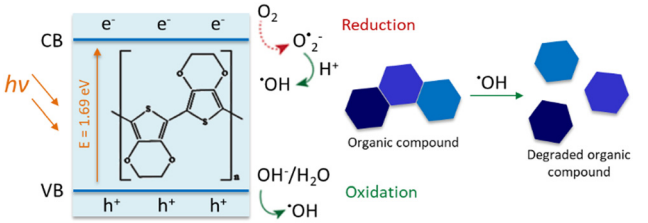


**Scheme 2** Schematic illustration of photocatalysis mechanism by E-PEDOT. The $e^-$ can be excited from VB to CB by the irradiation of PEDOT. The contaminants can be degraded through the subsequent oxidation and the formation of ˙OH.

*3.2.1.5. Reusability of E-PEDOT.* The reusability and stability of photocatalysts should be considered for their practical applications. Hence, in this study, the adsorption and photocatalytic activity of E-PEDOT were evaluated towards hexazinone removal after repeated use in 4 cycles. The experiments were carried out for 3 h in the dark (Dark 1st 3 h) followed by 3 h UV irradiation. The control experiments were also continued for another 3 h in the dark (Dark 2nd 3 h) to differentiate between the adsorption and photocatalytic activity of the catalyst. As depicted in Fig. 7, there was a decrease in E-PEDOT adsorption efficiency from cycle 1 to cycle 4 during the initial 3 h in the dark. Although hexazinone adsorption decreased further during the subsequent 3 h, it revealed lower adsorption compared to the first 3 h in cycles 3 and 4. This can be attributed to the saturation of the E-PEDOT surface by hexazinone molecules in cycles 3 and 4, which may lead to hexazinone desorption and result in a higher concentration of hexazinone in the solution.

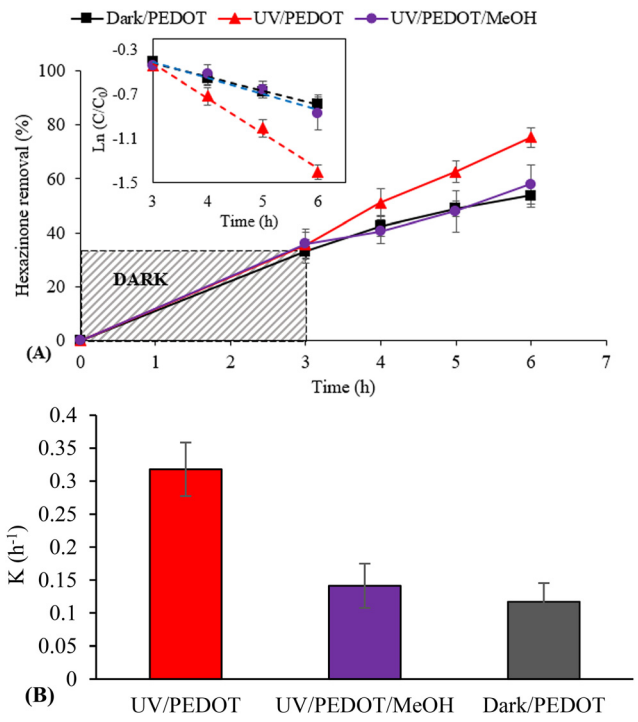


**Fig. 6** (A) Hexazinone removal (%) and kinetics in the presence of MeOH; (B) effect of MeOH on photodegradation rate of hexazinone (experimental conditions: $[hexazinone]_0$ = 5 μM, $[MeOH]_0$ = 0.5 mM, pH ~6.5, UVC intensity = 20 mW $cm^{-2}$).

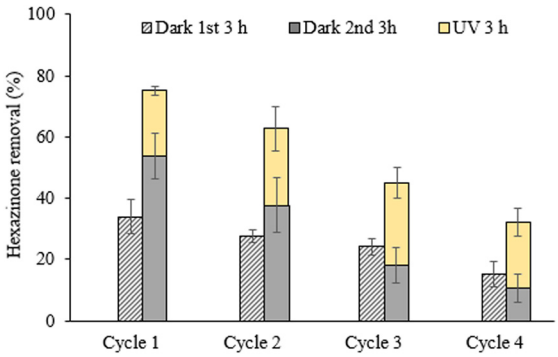


**Fig. 7** The reusability of E-PEDOT for hexazinone removal in the dark and under UV irradiation (experimental conditions: $[hexazinone]_0$ = 5 μM, pH ~6.5, UVC intensity = 20 mW $cm^{-2}$).

It has been reported that UV exposure can induce structural changes in PEDOT, leading to its instability and consequently lower photocatalytic activity.[11] However, in this study, the photocatalytic efficiency of E-PEDOT for hexazinone degradation remained relatively consistent (ranging from 21% to 26%) through each cycle. It should be noted that two different E-PEDOT strips were used to account for any differences between the photocatalytic activity and adsorption properties of E-PEDOT after 6 h. In addition, the FTIR and Raman characterisation results showed no change in E-PEDOT before and after irradiation (Fig. 3B, C, E, and F). Several studies reported good reusability of conducting polymers-based photocatalysts with minimal loss of reactivity.[50,51]

**3.2.2. Effect of C-PEDOT.** Chemical polymerisation of C-PEDOT using $FeCl_3$ as an oxidant makes it impossible to test its photocatalytic activity without the use of iron. In this study, C-PEDOT was used in powder form and immobilised on the electrospun fibre mat. The chacterisation of both C-PEDOT forms has been detailed elsewhere.[11] Hexazinone removal by these C-PEDOT samples is shown in Fig. 8. The immobilised C-PEDOT showed about 75% hexazinone degradation under 72 J $cm^{-2}$ UVC irradiation. We believe this degradation (%) can be due to the photocatalytic activity of not only the immobilised C-PEDOT but also Fe(III). The results of iron concentrations in the solutions indicated that a higher concentration of iron was leached into the solution under irradiation (15.5 ± 0.14 μM) compared to that in the dark condition (5.4 ± 1.2 μM).

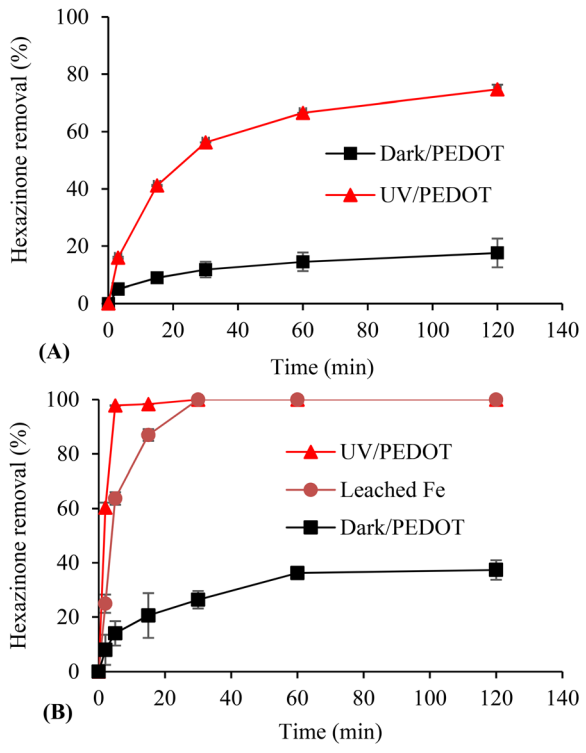


Fig. 8 Hexazinone removal (%) in the presence of (A) immobilised C-PEDOT and (B) C-PEDOT powder (experimental conditions: $[hexazinone]_0$ = 5 μM, C-PEDOT powder dosage = 0.5 g $L^{-1}$ pH ~6.5, UVC intensity = 20 mW $cm^{-2}$).

E-PEDOT with a similar size to immobilised C-PEDOT was also evaluated. The results revealed a significant adsorption of hexazinone (~95%), which makes it difficult to distinguish its photocatalytic effect (Fig. S5†). Meanwhile the adsorption capacity of the immobilised C-PEDOT was only 18%. Moreover, C-PEDOT powder demonstrated complete hexazinone degradation after 30 min of irradiation and 37% hexazinone removal in the dark after 1 h. Similar to the immobilised C-PEDOT, a higher concentration of iron (88 μM) was leached into the solution under irradiation than that in the dark (54 μM), although the immobilised C-PEDOT and C-PEDOT powder were thoroughly washed several times (>2 h) with MeOH to eliminate the salt. The higher amount of leached iron from C-PEDOT powder can be attributed to the structure of PEDOT, which can trap a higher amount of iron in the powder form. Hence, the potential leaching of iron should be taken into account when preparing photocatalysts using an iron source as an oxidant and/or dopant. In this study, the effect of leaching iron was tested by irradiating C-PEDOT powder in Milli-Q water at different contact times, followed by filtration of the solution to remove C-PEDOT. Hexazinone was added to the filtered solution and the solution was exposed to UV irradiation. As shown in Fig. 8B, the iron leached from C-PEDOT showed a significant contribution to the photocatalytic degradation of hexazinone. It is important to note that in Fig. 8B, the leached iron data still depict the percentage removal of hexazinone in a solution where C-PEDOT powder was irradiated in Milli-Q water for varying durations, followed by filtration to eliminate the C-PEDOT. Thus, it was only the leached iron in the solution from C-PEDOT which was present for the photocatalytic experiment. Subsequently, hexazinone was introduced into this filtered solution and exposed to UV irradiation.

Furthermore, to compare the photocatalytic effect of powdered C-PEDOT and E-PEDOT, the amount of E-PEDOT coated on the surface of CF (0.015 g) was compared with the amount of C-PEDOT powder (0.005 g) used for the experiments. The results demonstrated a significant superiority of the photocatalytic effect of C-PEDOT powder (Fig. 8B) over that of E-PEDOT (Fig. 5B), despite C-PEDOT powder being only one-third the amount of E-PEDOT. This difference could be attributed to the presence of iron in the powdered C-PEDOT. The use of iron can result in a higher photodegradation rate of contaminants due to the formation of additional $^{\bullet}OH$. It is also recommended to measure iron concentrations in aqueous solutions after photocatalysis using C-PEDOT.

### 3.3. Combination effect of Fe(III) and PEDOT

To understand the role of iron in the photocatalytic degradation efficiency of PEDOT, the experiments were carried out using two different methods. First, Fe(III) was

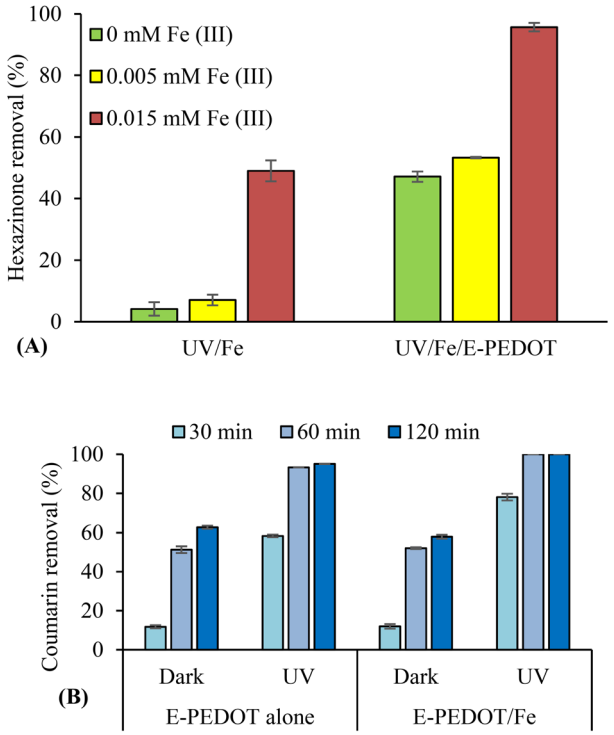


**Fig. 9** (A) Effect of $FeCl_3$ in the presence and absence of E-PEDOT under irradiation (experimental conditions: $[hexazinone]_0$ = 5 μM, $[Fe(III)]_0$ = 0.005 and 0.015 mM, pH ~6.5, irradiation time = 60 min, UVC intensity = 20 mW $cm^{-2}$); (B) coumarin removal in the dark and under irradiation in the presence of E-PEDOT and 0.05 mM $FeCl_3$.

added to the hexazinone solution in the presence of E-PEDOT at pH ~6.5. For these experiments, the samples containing two different concentrations of iron were kept in the dark for 3 h (Fig. 9A and S6†). The control experiments showed that the addition of Fe(III) had no effect on hexazinone adsorption onto E-PEDOT in the dark (Fig. S6†). Moreover, under irradiation, an additive effect on hexazinone degradation was observed in the UV/E-PEDOT/Fe system, demonstrating a combined effect of UV/E-PEDOT and UV/Fe systems. Hence, enhanced degradation in the UV/E-PEDOT/Fe process can be attributed to the presence of more reactive species, in particular, $^{\bullet}OH$, produced separately from E-PEDOT and Fe(III) under illumination. To prove the formation of more $^{\bullet}OH$ in the UV/E-PEDOT/Fe system, the removal of coumarin was tested in the presence of E-PEDOT alone and E-PEDOT in the presence of 0.05 mM $FeCl_3$ (Fig. 9B). As shown, coumarin adsorption is similar in both systems. However, its degradation is higher in the UV/E-PEDOT/Fe system (78–100%) than in the UV/E-PEDOT system (58–95%), proving the formation of a higher amount of $^{\bullet}OH$ in the UV/E-PEDOT/Fe system. The formation of 7-hydroxycoumarin with insignificant concentrations was observed only under irradiation, which might be due to its degradation after 5 min.[32]

In this study, iron concentration after treatment was measured by MP-AES and found to be the same as its initial concentration in the solution. The conversion of Fe(III) to Fe(II) has also been investigated in the presence of E-PEDOT (Fig. S7†). The concentration of Fe(III) (0.074 mM) was chosen for the complete degradation of hexazinone. Yang *et al.* stated the formation of $e^-$ and $h^+$ by irradiation of poly(EDOT–pyridazine–EDOT) polymer and Fe(III) in the solution of contaminants followed by their conversion to Fe(II) and Fe(IV), which can finally form $^{\bullet}OH$ and $O_2^{\bullet-}$ as well as Fe(III).[24] However, similar to the UV/Fe system (section 3.1 and Fig. 2B and C), the UV/E-PEDOT/Fe system also showed a higher Fe(II)% under irradiation than in the dark. Similar results were also observed in the presence and absence of E-PEDOT and the contaminant.

In a separate experiment, E-PEDOT strips were dipped in 1 M $FeCl_3$ solution, washed by immersion in Milli-Q water for 5, 10, 20, and 30 min to eliminate unbound salt, and then used for experiments with Milli-Q water in the dark and under irradiation for 3 h. After that, the residual iron was measured in the solutions (Table 1). Similar to the previous experiments, Fe(II) concentration was found to be higher under irradiation. Moreover, the average residual concentrations of iron under irradiation and in the dark were 18.04 and 8.25 μM, respectively (Table 1). The fact that a higher amount of iron leached out of the strip under irradiation than that in the dark can be due to the exposure of E-PEDOT strips to the irradiation.

Several studies developed novel photocatalysts using ferric salts for the degradation of organic contaminants from an aqueous solution.[11,17,47,51–54] For example, $Fe_3O_4$ introduction into PEDOT/CdS heterojunction enhanced the transfer of photoexcited electrons; thereby, the photocatalytic activity of the magnetic imprinted PEDOT/CdS heterojunction was greatly enhanced up to about 85%.[53] In another study, the synthesis of a photocatalyst using $Fe_2O_4$ and PEDOT (Z-scheme imprinted $ZnFe_2O_4$/Ag/PEDOT) *via* microwave polymerisation technique and surface imprinting method demonstrated ~72% degradation of tetracycline under 120 min simulated sunlight irradiation.[52] Yang *et al.* also highlighted the impact of Fe ions present in the matrix of poly(EDOT–pyridazine–EDOT) polymer in improving the polymer photocatalytic activity. In their study, an 8 : 1 ratio of $FeCl_3$ to polymer displayed the highest photodegradation efficiency (~95%) for methyl violet dye under visible irradiation for 300 min. This phenomenon was explained by narrowing the bandgap of the polymer by a small amount of Fe and hence postponing the $e^-/h^+$ pair recombination, beneficial for the photocatalytic performance of the

**Table 1** The average concentrations of residual iron (μM) leached from E-PEDOT strips dipped in 1 M Fe(III) into Milli-Q water solutions after 3 h

| Wash time (min) | Fe(III) concentration (μM) | |
|---|---|---|
| | UV irradiation | Dark |
| 5 | 21.24 ± 0.45 | 10.74 ± 0.26 |
| 10 | 19.83 ± 0.29 | 9.43 ± 0.55 |
| 20 | 17.87 ± 3.33 | 7.83 ± 0.5 |
| 30 | 13.2 ± 0.34 | 5 ± 0.52 |

polymer.[24] Moreover, Poulopoulos *et al.* found that the addition of Fe(III) could significantly enhance the removal of total carbon in the UV/$H_2O_2$ system, while the addition of $TiO_2$ showed no further efficiency in the removal of total carbon.[55] In another study, the addition of Fe(III) was found to increase the photocatalytic efficiency of $TiO_2$ by transferring the holes to the $TiO_2$ surface and their reaction with $OH^-$ for the formation of $^{\bullet}OH$.[56] Based on the literature and the results of the present study, we can conclude that the formation of $^{\bullet}OH$ from iron and PEDOT serves as the main mechanism driving the enhanced degradation of contaminants.

However, if iron ions are not immobilised, they may leach into the solution. A new procedure of ion imprinting was introduced to immobilise the iron ions on the surface of the $TiO_2$/fly-ash cenosphere catalyst, resulting in the efficient mutual transformation between Fe(III) and Fe(II). This method increased the separation rate of $e^-$ and $h^+$ in the cycling system and, hence, improved the photocatalytic performance of the catalyst.[57] This method was tried for the immobilisation of iron on the surface of E-PEDOT in this study; however, leaching of iron was still observed. The immobilisation of iron ions on the surface of E-PEDOT used in this study is proposed as an efficient method for the degradation of contaminants from water and wastewater. The presence of iron assisted the UV/E-PEDOT system in hexazinone degradation due to the formation of more $^{\bullet}OH$ in the solution. Compared to E-PEDOT in the absence of $FeCl_3$ with about 53% adsorption of hexazinone, a decrease in the adsorption behaviour (only 21.7% after 6 h) of E-PEDOT dipped in $FeCl_3$ solution was observed (Fig. S8†). It is hypothesised that this decrease can be due to the iron trapped in the E-PEDOT strip and blocking the adsorption sites on E-PEDOT, which makes it less available for hexazinone adsorption. Insignificant adsorption behaviour of chemically polymerised PEDOT has also been observed in the literature.[11,48] However, there was an increase in the photocatalytic degradation of hexazinone (100%) that was due to the presence of iron in the solution (Fig. S8†). Furthermore, a higher amount of Fe(III) (0.06 mM) leached into the solution under irradiation than in the dark (0.02 mM). Therefore, it can be concluded that iron addition, in general, to the photocatalyst system can increase the photocatalytic activity by producing OH radicals.

### 3.4. Photocatalytic degradation by-products of hexazinone and MB

The irradiated samples of hexazinone and MB were analysed by LC–MS/MS to determine their generated by-products in the presence of E-PEDOT and iron separately, using the MS full scan and spectra. The photocatalytic degradation of hexazinone (20 μM) and MB (16 μM) was carried out under 6.5 mW $cm^{-2}$ UV intensity. The samples obtained after 2 min and 60 min of the photocatalytic degradation at neutral pH were analysed. The peak intensity of the parent molecules decreased with increasing exposure time, implying their degradation. The following $M^+$ peaks of hexazinone fragments were identified in the presence of E-PEDOT in the MS/MS: *m*/*z* 223, 237, 239, 241, 255, and 267. These intermediates were also identified in hexazinone photodegradation in UV/$H_2O_2$ [7] and UV/$TiO_2$ [58] systems, and in its electrochemical degradation with a Bi-doped $PbO_2$ electrode.[59] The possible photocatalytic degradation pathway of hexazinone in the presence of PEDOT is expected to be similar to the pathway presented in these studies (Fig. 10) due to the dominant role of $^{\bullet}OH$ in the degradation of hexazinone by E-PEDOT. Moreover, the fragments of MB photocatalytic degradation at *m*/*z* 136 and 270 were identified in the presence of E-PEDOT and confirmed with the literature.[60] In the presence of 0.5 mM $FeCl_3$ but without E-PEDOT, by-products with *m*/*z* 257, 260, 285, 288, 328, and 385 were detected by photodegradation of hexazinone. Moreover, the degradation by-products of MB with *m*/*z* 120, 140, 160, 166, 193, 195, 236, 238, 262, 286, 302, 316, and 330 were determined in the presence of iron.

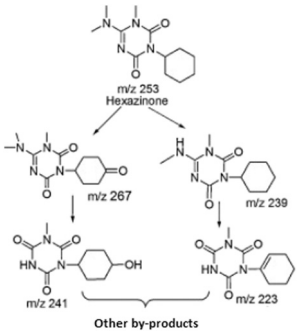


**Fig. 10** Hexazinone's possible photocatalytic degradation pathway (adapted from Mei *et al.* (2012)[58]).

## 4. Conclusions

Traditional photocatalysts, primarily effective under UV irradiation, pose significant limitations for large-scale treatment due to their high cost and impracticality in powder form, resulting in separation difficulties downstream of the treatment. However, a promising alternative lies in the utilisation of CP-based photocatalysts, which are non-toxic, cost-effective, and active under visible light, making them superior choices for the degradation of organic contaminants through photocatalysis. In this study, conducting polymer PEDOT was used as a photocatalyst. The effect of PEDOT separately and in combination with iron was studied. The study results demonstrated that iron enhanced the photochemical degradation of hexazinone and MB under irradiation with visible and UV wavelengths. The use of ferric salts under irradiation is suggested for the treatment of water and wastewater as a cost-effective process for the degradation and/or mineralisation of pollutants. Moreover, E-PEDOT showed photocatalytic activity of its own and without iron. The results of this study confirm the promising nature of the

immobilised E-PEDOT in the photocatalytic degradation of organic contaminants resistant to photolysis. The use of methanol as an $^{\bullet}OH$ quencher revealed the significant role of $^{\bullet}OH$ in both scenarios. In addition, the role of $^{\bullet}OH$ in UV/Fe, UV/E-PEDOT, and UV/E-PEDOT/Fe systems was proved by coumarin degradation. The recyclability of E-PEDOT showed a decrease in its adsorption properties, while its photocatalytic activity remained consistent during the 5 cycles.

Furthermore, the role of iron on the contaminant removal efficiency of PEDOT was investigated by performing the experiments in two different ways. First, the external addition of iron to the E-PEDOT system showed an increase in the photodegradation of contaminants without any effect on the adsorption properties of PEDOT. Second, dipping the E-PEDOT strips in iron solution revealed an increase in the photocatalytic activity of PEDOT that can be attributed to the presence of Fe(III) leaching into the solution from PEDOT strips. The results showed that even washing these strips with ethanol and water several times, as suggested in the literature, cannot completely eliminate the ferric chloride, usually used as an oxidant and/or dopant, from the strip. Iron showed an additive role in the photocatalytic activity of E-PEDOT. Thus, for the first time, it was shown that C-PEDOT photocatalytic efficiencies reported in the literature have two components, and the roles of iron and pure PEDOT were clearly distinguished.

Iron is frequently used for chemical polymerisation as an oxidant, dopant, or transient metal and has never been investigated prior to this study for its contribution to photocatalysis by PEDOT. However, introducing free iron in water at such a high concentration is not practical since iron has a secondary MCL of 0.3 mg $L^{-1}$. Instead, immobilisation on a suitable substrate, such as PEDOT, may be a more effective and viable approach. Our results also indicate a possible avenue to explore other cost-effective photocatalytic materials involving iron. The findings of this study provide valuable insights for future research in fine-tuning and optimising the amount of iron within the matrix of PEDOT. This optimisation yields highly promising photocatalysts for water treatment, thereby facilitating green and sustainable development. The immobilisation of iron on the surface of conducting polymers such as PEDOT is recommended for future study.

## Conflicts of interest

There are no conflicts to declare.

## Acknowledgements

Tahereh Jasemizad would like to thank The University of Auckland for providing her PhD scholarship. The authors also acknowledge the Faculty Research Development Fund of the Faculty of Engineering, The University of Auckland. Special thanks to Professor Paul Kilmartin for his help and advice on iron conversion experiments and to Professor Xiao Su for his valuable comments on this work.

## References

1 R. Gogoi, A. Singh, V. Moutam, L. Sharma, K. Sharma, A. Halder and P. F. Siril, Revealing the unexplored effect of residual iron oxide on the photoreforming activities of polypyrrole nanostructures on plastic waste and photocatalytic pollutant degradation, *J. Environ. Chem. Eng.*, 2022, **10**, 106649.

2 M. Kwon, S. Kim, Y. Yoon, Y. Jung, T.-M. Hwang, J. Lee and J.-W. Kang, Comparative evaluation of ibuprofen removal by UV/$H_2O_2$ and UV/$S_2O_8^{2-}$ processes for wastewater treatment, *Chem. Eng. J.*, 2015, **269**, 379–390.

3 T. Jasemizad, L. Bromberg, T. A. Hatton and L. P. Padhye, Oxidation of betrixaban to yield N-nitrosodimethylamine by water disinfectants, *Water Res.*, 2020, **186**, 116309.

4 T. Jasemizad, L. Bromberg and L. P. Padhye, The fate of aqueous betrixaban during adsorption, photolysis, and advanced oxidation: Removal, kinetics, and reaction mechanisms, *J. Water Proc.engineering*, 2021, **44**, 102430.

5 T. Jasemizad, P. Sun and L. P. Padhye, Aqueous N-nitrosamines: Precursors, occurrence, oxidation processes, and role of inorganic ions, *Crit. Rev. Environ. Sci. Technol.*, 2022, **52**, 3604–3650.

6 A. Agüera and A. Fernandez-Alba, GC-MS and LC-MS evaluation of pesticide degradation products generated through advanced oxidation processes: An overview, *J. Anal.*, 1998, **26**, 123–130.

7 T. Jasemizad and L. Padhye, Removal of aqueous hexazinone using adsorption, photolysis, and UV/$H_2O_2$, *ACS Spring 2021 National Meeting & Expo*, 2021.

8 T. Jasemizad and L. P. Padhye, Photodegradation and adsorption of hexazinone in aqueous solutions: removal efficiencies, kinetics, and mechanisms, *Environ. Sci. Pollut. Res.*, 2022, **29**(32), 48330–48339.

9 M. M. Bello and A. A. A. Raman, Adsorption and Oxidation Techniques to Remove Organic Pollutants from Water, in *Green Adsorbents for Pollutant Removal: Fundamentals and Design*, ed. G. Crini and E. Lichtfouse, Springer International Publishing, Cham, 2018, pp. 249–300.

10 P. Kar, G. Sathiyan and R. K. Gupta, 7 – Reaction intermediates during the photocatalytic degradation of emerging contaminants under visible or solar light, in *Visible Light Active Structured Photocatalysts for the Removal of Emerging Contaminants*, ed. O. Sacco and V. Vaiano, Elsevier, 2020, pp. 163–193.

11 R. Kumar, A. Akbarinejad, T. Jasemizad, R. Fucina, J. Travas-Sejdic and L. P. Padhye, The removal of metformin and other selected PPCPs from water by poly(3,4-ethylenedioxythiophene) photocatalyst, *Sci. Total Environ.*, 2021, **751**, 142302.

12 C. B. Ong, L. Y. Ng and A. W. Mohammad, A review of ZnO nanoparticles as solar photocatalysts: Synthesis,

 

mechanisms and applications, *Renewable Sustainable Energy Rev.*, 2018, **81**, 536–551.
13 P. Gharbani, A. Mehrizad and S. A. Mosavi, Optimization, kinetics and thermodynamics studies for photocatalytic degradation of Methylene Blue using cadmium selenide nanoparticles, *npj Clean Water*, 2022, **5**, 34.
14 J. Hong, K. H. Cho, V. Presser and X. Su, Recent advances in wastewater treatment using semiconductor photocatalysts, *Curr. Opin. Green Sustainable Chem.*, 2022, **36**, 100644.
15 D. Floresyona, F. Goubard, P.-H. Aubert, I. Lampre, J. Mathurin, A. Dazzi, S. Ghosh, P. Beaunier, F. Brisset, S. Remita, L. Ramos and H. Remita, Highly active poly(3-hexylthiophene) nanostructures for photocatalysis under solar light, *Appl. Catal., B*, 2017, **209**, 23–32.
16 S. Taccola, F. Greco, A. Zucca, C. Innocenti, C. de Julián Fernández, G. Campo, C. Sangregorio, B. Mazzolai and V. Mattoli, Characterisation of Free-Standing PEDOT:PSS/Iron Oxide Nanoparticle Composite Thin Films and Application As Conformable Humidity Sensors, *ACS Appl. Mater. Interfaces*, 2013, **5**, 6324–6332.
17 S. Ghosh, N. A. Kouame, S. Remita, L. Ramos, F. Goubard, P.-H. Aubert, A. Dazzi, A. Deniset-Besseau and H. Remita, Visible-light active conducting polymer nanostructures with superior photocatalytic activity, *Sci. Rep.*, 2015, **5**, 18002.
18 S. Nie, Z. Li, Y. Yao and Y. Jin, Progress in synthesis of conductive polymer poly (3, 4-ethylenedioxythiophene), *Front. Chem.*, 2021, **9**, 1137.
19 Z. Cui, C. Coletta, R. Rebois, S. Baiz, M. Gervais, F. Goubard, P. H. Aubert, A. Dazzi and S. Remita, Radiation-induced reduction–polymerization route for the synthesis of PEDOT conducting polymers, *Radiat. Phys. Chem.*, 2016, **119**, 157–166.
20 N. S. Shah, X. He, J. A. Khan, H. M. Khan, D. L. Boccelli and D. D. Dionysiou, Comparative studies of various iron-mediated oxidative systems for the photochemical degradation of endosulfan in aqueous solution, *J. Photochem. Photobiol., A*, 2015, **306**, 80–86.
21 H. Wang, H. Yao, P. Sun, J. Pei, D. Li and C.-H. Huang, Oxidation of tetracycline antibiotics induced by Fe(III) ions without light irradiation, *Chemosphere*, 2015, **119**, 1255–1261.
22 P. Mazellier, J. Jirkovsky and M. Bolte, Degradation of Diuron Photoinduced by Iron (III) in Aqueous Solution, *Pestic. Sci.*, 1997, **49**, 259–267.
23 F. J. Benitez, J. L. Acero, F. J. Real, G. Roldan and F. Casas, Comparison of different chemical oxidation treatments for the removal of selected pharmaceuticals in water matrices, *Chem. Eng. J.*, 2011, **168**, 1149–1156.
24 L. Yang, R. Jamal, F. Liu, Y. Wang and T. Abdiryim, Structure and photocatalytic activity of a low band gap donor–acceptor–donor (D–A–D) type conjugated polymer: poly(EDOT–pyridazine–EDOT), *RSC Adv.*, 2017, **7**, 1877–1886.
25 T. Jasemi Zad, Oxidative degradation of betrixaban and hexazinone: kinetics, reaction mechanisms, and nitrogenous disinfection by-products formation potential, *PhD*, The University of Auckland, 2021.
26 T. Jasemizad and L. P. Padhye, Simultaneous analysis of betrixaban and hexazinone using liquid chromatography/tandem mass spectrometry in aqueous solutions, *MethodsX*, 2019, **6**, 1863–1870.
27 H. Yao, J. Pei, H. Wang and J. Fu, Effect of Fe(II/III) on tetracycline degradation under UV/VUV irradiation, *Chem. Eng. J.*, 2017, **308**, 193–201.
28 H. Park and W. Choi, Visible light and Fe(III)-mediated degradation of Acid Orange 7 in the absence of $H_2O_2$, *J. Photochem. Photobiol., A*, 2003, **159**, 241–247.
29 R. A. Larson, M. B. Schlauch and K. A. Marley, Ferric ion promoted photodecomposition of triazines, *J. Agric. Food Chem.*, 1991, **39**, 2057–2062.
30 A. Machulek Jr , F. H. Quina, F. Gozzi, V. O. Silva, L. C. Friedrich and J. E. Moraes, Fundamental mechanistic studies of the photo-Fenton reaction for the degradation of organic pollutants, *Organic pollutants ten years after the Stockholm convention-environmental and analytical update*, InTech, 2012, pp. 271–292.
31 T. Paul, P. L. Miller and T. J. Strathmann, Visible-Light-Mediated $TiO_2$ Photocatalysis of Fluoroquinolone Antibacterial Agents, *Environ. Sci. Technol.*, 2007, **41**, 4720–4727.
32 A. Moreira, A. C. Borges, B. B. de Souza, L. R. Barbosa, V. R. de Mendonca, C. D. Freschi and G. P. G. Freschi, Microwave discharge electrodeless mercury lamp (Hg-MDEL): an energetic, mechanistic and kinetic approach to the degradation of Prozac®, *J. Environ. Chem. Eng.*, 2019, **7**(2), 102916.
33 J. De Laat, H. Gallard, S. Ancelin and B. Legube, Comparative study of the oxidation of atrazine and acetone by $H_2O_2$/UV, Fe(III)/UV, Fe(III)/$H_2O_2$/UV and Fe(II) or Fe(III)/$H_2O_2$, *Chemosphere*, 1999, **39**, 2693–2706.
34 Y. Chen, H. Li, Z. Wang, T. Tao, D. Wei and C. Hu, Photolysis of Chlortetracycline in aqueous solution: Kinetics, toxicity and products, *J. Environ. Sci.*, 2012, **24**, 254–260.
35 N. Brand, G. Mailhot and M. Bolte, Degradation and photodegradation of tetraacetylethylenediamine (TAED) in the presence of iron (III) in aqueous solution, *Chemosphere*, 1997, **34**, 2637–2648.
36 C. Lee and J. Yoon, Determination of quantum yields for the photolysis of Fe (III)-hydroxo complexes in aqueous solution using a novel kinetic method, *Chemosphere*, 2004, **57**(10), 1449–1458.
37 T. Abdiryim, A. Ali, R. Jamal, Y. Osman and Y. Zhang, A facile solid-state heating method for preparation of poly(3,4-ethelenedioxythiophene)/ZnO nanocomposite and photocatalytic activity, *Nanoscale Res. Lett.*, 2014, **9**, 89.
38 J. Wang, S. Li, Q. Qin and C. Peng, Sustainable and feasible reagent-free electro-Fenton via sequential dual-cathode electrocatalysis, *Proc. Natl. Acad. Sci. U. S. A.*, 2021, **118**, 2108573118.
39 M. Al-Haik, C. C. Luhrs, M. M. Reda Taha, A. K. Roy, L. Dai, J. Phillips and S. Doorn, Hybrid Carbon Fibers/Carbon Nanotubes Structures for Next Generation Polymeric Composites, *J. Nanotechnol.*, 2010, 860178.

40 B. Gao, J. An, Y. Wang, L. Wang and M. Sillanpää, Comparative study of the photocatalytic, electrocatalytic and photoelectrocatalytic behaviour of poly(3,4-ethylenedioxythiophene), *J. Electroanal. Chem.*, 2020, **858**, 113742.

41 Z. Katančić, W.-T. Chen, G. I. N. Waterhouse, H. Kušić, A. Lončarić Božić, Z. Hrnjak-Murgić and J. Travas-Sejdic, Solar-active photocatalysts based on $TiO_2$ and conductive polymer PEDOT for the removal of bisphenol A, *J. Photochem. Photobiol., A*, 2020, **396**, 112546.

42 D. Weerakoon, B. Bansal, L. P. Padhye, A. Rachmani, L. J. Wright and G. S. Roberts, *et al.* A critical review on current urea removal technologies from water: An approach for pollution prevention and resource recovery, *Sep. Purif. Technol.*, 2023, **314**, 123652.

43 S. Khan and A. K. Narula, Ternary photocatalyst based on conducting polymer doped functionalised multiwall carbon nanotubes decorated with nanorods of metal oxide, *J. Mater. Sci. Eng. B*, 2019, **243**, 86–95.

44 B. Gao, S. Dong, J. Liu and M. Sillanpää, PEDOT:PSS decorated $ZnIn_2S_4$ for reduced recombination of photogenerated electron-hole pairs, *Mater. Lett.*, 2018, **224**, 64–66.

45 L. Zhang, C. Ni, H. Jiu, C. Xie, J. Yan and G. Qi, One-pot synthesis of Ag-$TiO_2$/reduced graphene oxide nanocomposite for high performance of adsorption and photocatalysis, *Ceram. Int.*, 2017, **43**, 5450–5456.

46 H. Huang, R. Cao, S. Yu, K. Xu, W. Hao, Y. Wang, F. Dong, T. Zhang and Y. Zhang, Single-unit-cell layer established $Bi_2WO_6$ 3D hierarchical architectures: Efficient adsorption, photocatalysis and dye-sensitised photoelectrochemical performance, *Appl. Catal., B*, 2017, **219**, 526–537.

47 G. Liu, J. Ma, X. Li and Q. Qin, Adsorption of bisphenol A from aqueous solution onto activated carbons with different modification treatments, *J. Hazard. Mater.*, 2009, **164**(2–3), 1275–1280.

48 S. Ghosh, N. A. Kouamé, L. Ramos, S. Remita, A. Dazzi, A. Deniset-Besseau, P. Beaunier, F. Goubard, P.-H. Aubert and H. Remita, Conducting polymer nanostructures for photocatalysis under visible light, *Nat. Mater.*, 2015, **14**, 505–511.

49 Z. Lu, Z. Yu, J. Dong, X. Xiong, L. Gao, M. Song, Y. Liu, D. Fan, Y. Yan and P. Huo, Enhanced photocatalytic activity and selectivity of a novel magnetic PW@ PEDOT imprinted photocatalyst with good reproducibility, *J. Nanotechnol.*, 2018, **13**, 1850020.

50 R. Nosrati, A. Olad and R. Maramifar, Degradation of ampicillin antibiotic in aqueous solution by ZnO/polyaniline nanocomposite as photocatalyst under sunlight irradiation, *Environ. Sci. Pollut. Res.*, 2012, **19**(6), 2291–2299.

51 Q. Zhou, Y. Wang, J. Xiao, H. Fan and C. Chen, Preparation and characterization of magnetic nanomaterial and its application for removal of polycyclic aromatic hydrocarbons, *J. Hazard. Mater.*, 2019, **371**, 323–331.

52 Z. Lu, Z. Yu, J. Dong, M. Song, Y. Liu, X. Liu, Z. Ma, H. Su, Y. Yan and P. Huo, Facile microwave synthesis of a Z-scheme imprinted $ZnFe_2O_4$/Ag/PEDOT with the specific recognition ability towards improving photocatalytic activity and selectivity for tetracycline, *Chem. Eng. J.*, 2018, **337**, 228–241.

53 Z. Lu, G. Zhou, M. Song, X. Liu, H. Tang, H. Dong, P. Huo, F. Yan, P. Du and G. Xing, Development of magnetic imprinted PEDOT/CdS heterojunction photocatalytic nanoreactors: 3-Dimensional specific recognition for selectively photocatalyzing danofloxacin mesylate, *Appl. Catal., B*, 2020, **268**, 118433.

54 L. Zhang, R. Jamal, Q. Zhao, M. Wang and T. Abdiryim, Preparation of PEDOT/GO, PEDOT/$MnO_2$, and PEDOT/GO/$MnO_2$ nanocomposites and their application in catalytic degradation of methylene blue, *Nanoscale Res. Lett.*, 2015, **10**, 148.

55 S. G. Poulopoulos, A. Yerkinova, G. Ulykbanova and V. J. Inglezakis, Photocatalytic treatment of organic pollutants in a synthetic wastewater using UV light and combinations of TiO2, $H_2O_2$ and Fe (III), *PLoS One*, 2019, **14**(5), e0216745.

56 Z. D. Meng, K. Zhang and W. C. Oh, Preparation of different Fe containing $TiO_2$ photocatalysts and comparison of their photocatalytic activity, *Han'guk Chaelyo Hakhoechi*, 2010, **20**(4), 228–234.

57 P. Huo, Z. Lu, H. Wang, J. Pan, H. Li, X. Wu, W. Huang and Y. Yan, Enhanced photodegradation of antibiotics solution under visible light with $Fe^{2+}$/$Fe^{3+}$ immobilised on $TiO_2$/fly-ash cenospheres by using ions imprinting technology, *Chem. Eng. J.*, 2011, **172**, 615–622.

58 M. Mei, Z. Du, R. Xu, Y. Chen, H. Zhang and S. Qu, Photocatalytic degradation of hexazinone and its determination in water via UPLC-MS/MS, *J. Hazard. Mater.*, 2012, **221–222**, 100–108.

59 Y. Yao, M. Li, Y. Yang, L. Cui and L. Guo, Electrochemical degradation of insecticide hexazinone with Bi-doped $PbO_2$ electrode: Influencing factors, intermediates and degradation mechanism, *Chemosphere*, 2019, **216**, 812–822.

60 H. Xiang, G. Ren, Y. Zhong, D. Xu, Z. Zhang, X. Wang and X. Yang, $Fe_3O_4$@ C nanoparticles synthesized by in situ solid-phase method for removal of methylene blue, *Nanomaterials*, 2021, **11**(2), 330.

 